Thermal Stability Analysis of Multiple Emitter Finger Microwave AlGaAs/GaAs Heterojunction Bipolar Transistors

L.L. Liou, B.Bayraktaroglu*, and C.I. Huang
Solid State Electronics Directorate
Wright Laboratory
Wright Patterson Air Force Base, OH 45433-7323
* North Carolina State University
College of Engineering
Raleigh, NC 27695

Abstract: We developed a numerical electro-thermal model for AlGaAs/GaAs heterojunction bipolar transistors (HBTs) taking into account the nonuniform junction temperature rise due to self-heating. The model simulates both the dc current-voltage (I-V) characteristics and microwave performance of multi-emitter finger devices. The linear active region of the common-emitter I-V characteristics exhibits "current crush", where the collector current rapidly decays with increasing collector voltage due to the formation of highly localized hot spots within the device. It was also shown that a rapid fall off in the cut-off frequency and maximum frequency of oscillation occurs corresponding to the onset of this thermal instability. Methods of overcoming this instability using emitter ballast resistors and higher thermal conductivity substrates were discussed with corresponding effects on dc and microwave performance of the device.

I. Introduction

GaAs-based heterojunction bipolar transistors (HBTs) have demonstrated significantly higher power output and power density at microwave frequencies than conventional FETs[1-3]. This performance advantage makes the HBT a strong candidate for transmitter power amplifier applications requiring high voltage, high current density, and high efficiency.

The high power density capability of HBTs stems from the low sheet resistance of the base layers and from the high electron mobility of GaAs, together, these factors allow high frequency operation above a current density of 5 x 10^4 A/cm^2 by avoiding the Webster and Kirk effects. Such high current density coupled with high collector voltages (based on collector layer design) produce an electronic performance limitation of HBTs to at least 5 x 10^5 W/cm^2 in the active area. However, this high power potential of HBTs is not realized in practical devices operating under CW conditions due to the poor thermal conductivity of GaAs and the onset of thermal instability caused by the negative temperature coefficient of the emitter-base junction turn-on voltage. Unless proper design precautions are employed in the design of multi-emitter finger power devices, nonuniform temperature distribution due to self-heating can result in thermal runaway, severely limiting the power potential of these devices.

To improve the power output of HBTs while providing better reliability, ballasting of the emitter-base junction and/or improving the device thermal resistance should be considered. Both of these options are used in Si bipolar transistors operating at low microwave frequencies. Prior to this report, the effectiveness of such solutions to GaAs HBTs has not been examined in detail by considering simultaneously the power dissipation improvements and the potential microwave performance degradation. Such analyses would be useful for establishing design guidelines for incorporating ballast resistors and thermal conductivity improvements.

In this study, we have analyzed the temperature distribution in a multi-emitter-finger power HBT due to self heating by considering the redistribution of current as a function of local temperature. With an appropriate model describing the base current density, current gain and power dissipation as functions of junction temperature, it was found that the collector current collapses in the transistor's common-emitter I-V characteristics. The dependence of the local hot spot formation on the emitter ballast resistor and substrate thermal conductivity was modeled. The cutoff frequency and maximum frequency of oscillation were also calculated by considering the nonuniform temperature and current density within the device. Results show that the microwave performance degradation can be substantial if the devices are stabilized by using the emitter ballast resistors only. Use of a high thermal conductivity substrate along with a moderate amount of emitter ballasting may prove to be a better approach for achieving high power and high performance in HBTs.

OF1

II. Model Description

The base and collector current densities of AlGaAs/GaAs HBT as functions of temperature can be calculated using the drift-diffusion model. Typical calculation and experimental results [4,5] of Gummel plots show a nearly constant negative temperature coefficient, δ, of base-emitter voltage, V_{be}, for a constant base current density. Including an emitter ballast resistance, the base current density, J_b, can be given by:

$$J_b(T) = J_{b0}\, e^{\frac{V_{be}-(\beta+1)J_b\rho_e+\delta(T-T_0)}{n_b kT_0/q}} \qquad (1)$$

where β is the current gain, ρ_e is the specific resistance at the emitter (unit = Ω-cm^2), k is the Boltzmann's constant, T and T_0 are the junction and heat sink temperatures, respectively, n_b is

the ideality factor for the base current density, and the J_{b0} is the pre-exponential factor. A typical HBT shows a decrease in the emitter injection efficiency as the temperature increases, and the current gain as a function of temperature can be given by:

$$\beta(T) = \beta_0 e^{\frac{\Delta E}{kT}} \tag{2}$$

where ΔE is the activation energy, also referred to as "apparent" valence band discontinuity [4,5,8], and β_0 is the pre-exponential factor. The heat dissipation density of the device is given by:

$$p(T) = \beta(T) J_b(T) V_{ce} \tag{3}$$

where V_{ce} is the collector-emitter voltage.

Transit time analysis was used to calculate the cut-off frequency. The multi-emitter finger HBT was treated as composed of a number of unit cells. Each unit cell had a constant, but slightly differently junction temperature. Because of the nonuniform temperature distribution, each unit cell has a different cut-off frequency. At i-th cell, the cut-off frequency, f_t^i is given by:

$$f_t^i = \frac{1}{2\pi\tau_{ec}^i} \tag{4}$$

where τ_{ec}^i is the total transit time, which is the summation of the base-emitter junction charging time (τ_e), the collector-base junction charging time (τ_c), the base transit time (τ_b) and the transit time through the collector depletion region (τ_{sv})[8]. The small signal current gain as a function of frequency, ν, is $\beta^i(\nu)$, which is given by:

$$\beta^i(\nu) = \frac{\alpha_0^i}{(1-\alpha_0^i) + j\frac{\nu}{f_t^i}} \tag{5}$$

where α_0^i is the dc common-base small signal current gain at i-th unit cell; its relation with β_0^i, the dc common-emitter small signal current gain at i-th unit cell, is given by:

$$\alpha_0^i = \frac{\beta_0^i}{1+\beta_0^i} \tag{6}$$

The total small signal current gain is then given by:

$$\beta(\nu) = \frac{I_c}{I_b} = \frac{\sum_i \beta^i(\nu) J_b^i A_i}{\sum_i J_b^i A_i} \tag{7}$$

where A_i is the area of i-th unit cell.

The maximum oscillation frequency, f_{max}, is calculated from the frequency dependence of maximum available gain, G_{max}, which is given by:

$$G_{max} = \frac{f_t}{8\pi Re(Z_{BB}) C_{bc} \nu^2} \tag{8}$$

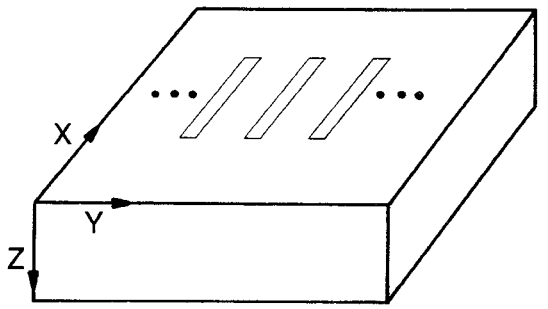

Fig. 1 Schematic diagram of the multi-emitter fingers on GaAs Chip.

where C_{bc} is the base-collector capacitance including the junction beneath the base metal pads. With the distributed transmission line model[9], the impedance due to the base metal pads is given by:

$$Z_{BB} = L_B R \frac{\coth\{L_B R[(G+j\omega c)/R]^{0.5}\}}{L_B R[(G+j\omega c)/R]^{0.5}} \tag{9}$$

where L_B is the length of the base metal pad, 1/G, R and C are the specific base contact resistance, base sheet resistance and base contact capacitance per unit area, respectively.

III. Numerical Results and Discussions

Fig. 1 shows a schematic diagram of an AlGaAs/GaAs HBT device with multiple emitter fingers fabricated on a 500×500×75 μm^3 GaAs substrate. The emitter areas on the GaAs substrate were considered as nonuniform heat sources. The temperature distribution was obtained by solving the heat transfer equation with proper boundary conditions. An iterative numerical scheme was used to obtain a self-consistent solution of both the temperature and current density distributions.

A device with 3 emitter fingers, located at the center of the top surface, was used to demonstrate the temperature effects on the dc and rf device performance. Each emitter finger has an area of 2×10 μm^2 and the separation between fingers is 10 μm. A unit cell sample area of 1×1 μm^2 was used in the calculation. The bottom surface is assumed to be at the heat sink temperature of T_0=300K. The device parameters used in the calculation are: n_b=3, ΔE=0.07 eV, and current gain at T_0 is 20.

Fig. 2 shows the calculated common-emitter I-V and the f_t and f_{max} vs. V_{ce} with base currents of 0.5, 1, 1.5 and 2 mA, and a zero ballast emitter resistance. As V_{ce} increases, the collector current decreases initially caused by the reduction of current gain at a higher junction temperatures. As V_{ce} continues to increase, the current suddenly crushes to a smaller value. The temperature distributions on the top surface of the chip are shown in Figs. 3(a), (b), (c) and (d) for the cases of I_b = 1 mA and V_{ce} = 4, 6, 8, and 10 V, respectively. Prior to the current crush (V_{ce} = 4 and 6 V) the temperature variations are small across the 3 emitter fingers. At and after the current crush (V_{ce} = 8 and 10 V), the temperature distributions show

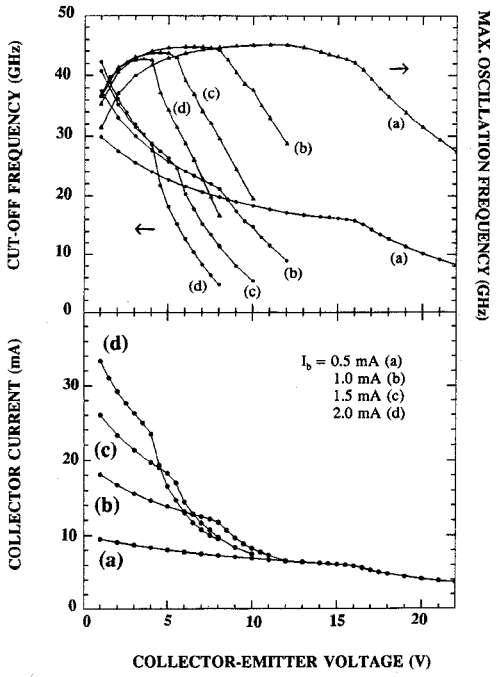

Fig. 2 Calculated collector current (•), cut-off frequency (•) and maximum oscillation frequency (▲) vs. V_{ce} for ρ_e = 0, K_s = 0.467 W/(cm-K) and I_b = 0.5, 1.0, 1.5 and 2.0 mA.

drastic differences between the center and the other two emitter fingers (please note the change in vertical scale). As V_{ce} is increased, the center finger eventually conducts most of the base current, and the other two become nearly inactive. The collector current continues to decrease due to a smaller current gain at a higher junction temperature. The crush occurs at a constant power of 92 mW in this case.

It is also seen in Fig. 2 that before the current crushes, f_t declines gradually as V_{ce} increases. The rate of decline of f_t is larger in the V_{ce} range where the collector is partially depleted, compared to that in the V_{ce} region where the collector is completely depleted. As V_{ce} increases further, a fall-off of the cut-off frequency occurs coinciding with the collector current crush. The reason is that when the current crush occurs, a large portion of the collector current flows through a small emitter area (hot spot) and lowers the current density elsewhere. These nearly inactive emitter areas have large dynamic emitter resistances. Consequently, the average f_t of the HBT declines further in addition to the decrease resulting from the increase in local temperature. The f_{max} increases initially with V_{ce}, due to the reduction of base-collector junction capacitance. The f_{max} reaches a saturation value before the current crush point is reached, where a rapid fall-off is observed similar to the behavior of f_t vs. V_{ce}.

Fig. 4 shows both the dc characteristics and microwave performance as affected by the presence of emitter ballast resistance (ρ_e). As ballast resistance increases, the current instability threshold increases, while f_t and f_{max} decrease due to a larger emitter charging time. These results clearly indicate a trade-off between the power and frequency performances.

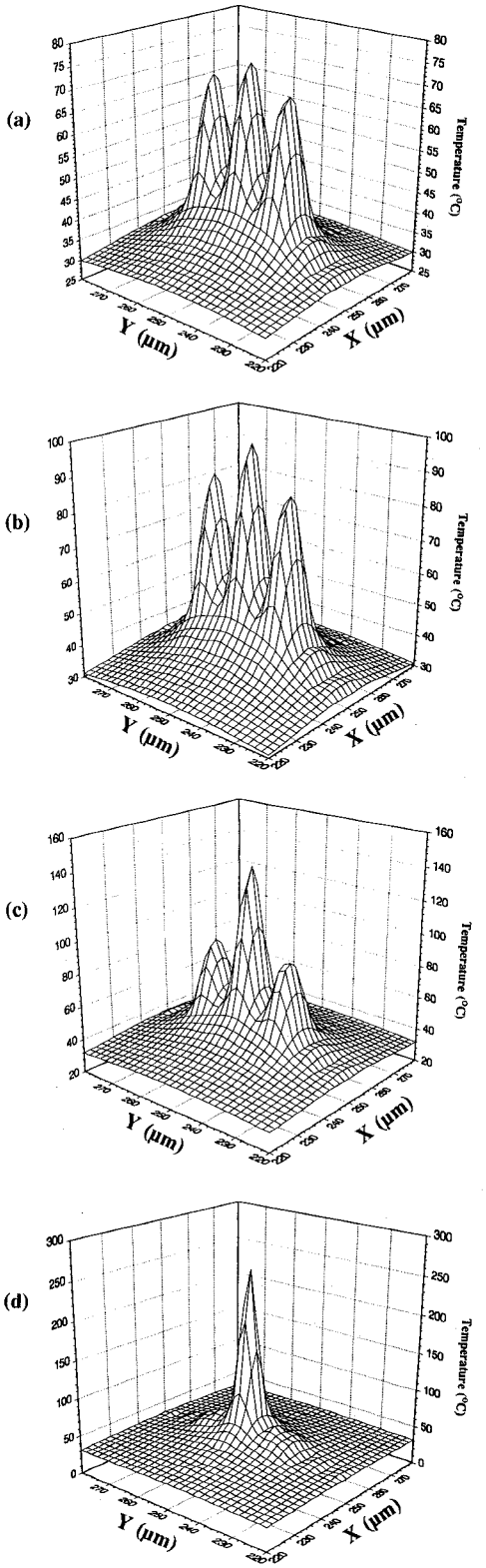

Fig. 3 Temperature distributions on the surface of the chip for I_b = 1 mA and V_{ce} = 4 V (a), 6 V (b), 8 V (c) and 10 V (d).

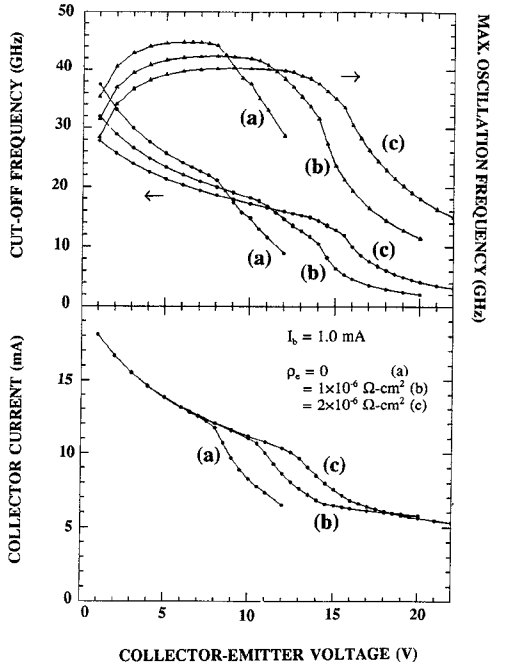

Fig. 4 Calculated collector current (•), cut-off frequency (•) and maximum oscillation frequency (▲) vs. V_{ce} for ρ_e = 0, 1 and 2×10^{-6} Ω-cm^2, K_s = 0.467 W/(cm-K) and I_b = 1.0 mA.

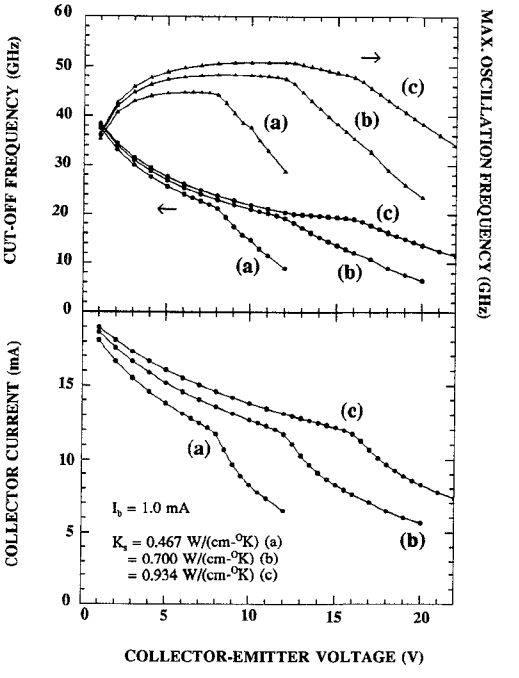

Fig. 5 Calculated collector current (•), cut-off frequency (•) and maximum oscillation frequency (▲) vs. V_{ce} for ρ_e = 0, K_s = 0.467, 0.700 and 0.934 W/(cm-K) and I_b = 1.0 mA.

Fig. 5 shows both the dc characteristics and microwave performance as functions of V_{ce} with substrate thermal conductivity (K_s) as a variable parameter. The power threshold of the current instability increases almost linearly with the substrate thermal conductivity. It is also shown that due to a smaller temperature increase in the case of having a larger thermal conductivity substrate, the magnitude of the negative differential resistance in the dc characteristics as well as the f_t and f_{max} degradation rates are reduced.

IV. Conclusions

In this paper, we studied the simulated characteristics of multiple-emitter finger AlGaAs/GaAs HBTs in terms of dc I-V, f_t, and f_{max}. Because of the self-heating effect, the device shows collapse in both dc and rf performance when dc power increases to a threshold. This threshold limits the power capability of conventional HBTs. Its dependence on the emitter ballast resistance and substrate thermal conductivity can be determined by the present model, and the ballasting requirement for optimum power and microwave performance may be established.

References:

[1] M.A. Khatibzadeh, B. Bayraktaroglu and T. Kim, "12 W monolithic X-band HBT power amplifier," IEEE Microwave and Millimeter Wave Monolithic Circuit Symp. Tech. Dig., pp. 47, 1992.

[2] M. G. Adlerstein, et. al., "High power density pulsed X-band heterojunction bipolar transistor," Electronics Lett. vol. 27, pp. 148, 1991.

[3] J.A. Higgins, "GaAs heterojunction bipolar transistors: A second generation microwave power amplifier transistor," Microwave Journal, pp. 176, May 1991.

[4] L. L. Liou, C. I. Huang and J. Ebel, "Numerical studies of thermal effects on heterojunction bipolar transistor current-voltage characteristics using one-dimensional simulation," Solid-State Electronics vol. 35, pp. 579-585, 1992.

[5] M. G. Adlerstein and M. P. Zaitlin, "Thermal resistance measurement for AlGaAs/GaAs heterojunction bipolar transistors," IEEE Trans. on Electron Device, vol. ED-38, pp. 1553-1554, 1991.

[6] G-B Gao, et. al., "Thermal design studies of high-power heterojunction bipolar transistors," IEEE Trans. on Electron Devices, vol. ED-36, pp. 854-862, 1989.

[7] J. R. Waldrop, K. C. Wang and P. M. Asbeck, "Determination of junction temperature in AlGaAs/GaAs heterojunction bipolar transistors by electrical measurement," IEEE Trans. on Electron Devices, vol. 39, pp. 1248-1250, 1992.

[8] A. B. Phillips, "Transistor engineering and introduction to integrated semiconductor circuits," McGraw-Hill Book Co., Inc., New York, 1962.

[9] W. Liu, D. Costa and J. S. Harris Jr, "A simplified model for the distributed base contact impedance in heterojunction bipolar transistors," Solid-State Electronics, vol. 35, pp. 547-552, 1992.